

# Mortaring for linear elasticity using low order finite elements

Tom Gustafsson<sup>1</sup>, Peter Råback<sup>1</sup>, Juha Videman<sup>1</sup>

---

## Abstract

We introduce a stabilized mortar method for linear elasticity and compare it to the standard mixed mortar method without stabilization. We present the stability criteria of the lowest order mixed approximation and investigate its use for tie contact problems. Our numerical results demonstrate the stability and the convergence of the methods. Moreover, the results show that the low order mixed method can be successfully extended to three dimensions.

---

## 1. Introduction

Mortaring via Lagrange multipliers is also a prototype of elastic contact problems besides its use in domain decomposition. Consider, for example, a linear elastic body  $\Omega \subset \mathbb{R}^d$ ,  $d = 2, 3$ , with the displacement field  $\mathbf{u} : \Omega \rightarrow \mathbb{R}^d$  and body loading  $\mathbf{f} : \Omega \rightarrow \mathbb{R}^d$ . In the absence of other external forces, the principle of virtual work reads as follows:

$$\int_{\Omega} \boldsymbol{\sigma}(\mathbf{u}) : \boldsymbol{\varepsilon}(\delta \mathbf{u}) \, d\Omega = \int_{\Omega} \mathbf{f} \cdot \delta \mathbf{u} \, d\Omega,$$

where  $\boldsymbol{\varepsilon}(\mathbf{w}) = \frac{1}{2}(\nabla \mathbf{w} + \nabla \mathbf{w}^T)$  is the infinitesimal strain tensor and  $\boldsymbol{\sigma}(\mathbf{w}) = \mathcal{C} : \boldsymbol{\varepsilon}(\mathbf{w})$  is the linear elastic stress tensor corresponding to the fourth-order constitutive tensor  $\mathcal{C}$ . Suppose now that  $\Omega$  is split into two parts  $\Omega_1$  and  $\Omega_2$  with the displacements  $\mathbf{u}_1$  and  $\mathbf{u}_2$ , respectively. The continuity across the interface  $\Gamma = \partial\Omega_1 \cap \partial\Omega_2$  can be enforced using a Lagrange multiplier field  $\boldsymbol{\lambda} : \Gamma \rightarrow \mathbb{R}^d$  through the saddle point formulation

$$\begin{cases} \int_{\Omega_1} \boldsymbol{\sigma}(\mathbf{u}_1) : \boldsymbol{\varepsilon}(\delta \mathbf{u}_1) \, d\Omega & + \int_{\Gamma} \boldsymbol{\lambda} \cdot \delta \mathbf{u}_1 \, d\Gamma = \int_{\Omega_1} \mathbf{f} \cdot \delta \mathbf{u}_1 \, d\Omega \\ \int_{\Omega_2} \boldsymbol{\sigma}(\mathbf{u}_2) : \boldsymbol{\varepsilon}(\delta \mathbf{u}_2) \, d\Omega - \int_{\Gamma} \boldsymbol{\lambda} \cdot \delta \mathbf{u}_2 \, d\Gamma = \int_{\Omega_2} \mathbf{f} \cdot \delta \mathbf{u}_2 \, d\Omega \\ \int_{\Gamma} \delta \boldsymbol{\lambda} \cdot \mathbf{u}_1 \, d\Gamma & - \int_{\Gamma} \delta \boldsymbol{\lambda} \cdot \mathbf{u}_2 \, d\Gamma = 0. \end{cases} \quad (1)$$

In contact mechanics, the linear saddle point formulation (1) corresponds to a single contact iteration with zero initial gap between the bodies  $\Omega_1$  and  $\Omega_2$ . In fact, the stability results carry over to the variational inequality formulations. Formulation (1) is sometimes referred to as *tie contact problem*.

In principle, the Lagrange multiplier formulation can accommodate nonmatching computational meshes and even different finite element spaces over  $\Gamma$ , and, thus, can be made quite generic with respect to the discretization of parts  $\Omega_1$  and  $\Omega_2$ . However, it is well known [1] that such saddle point system is stable only if a certain compatibility criterion, the Babuška–Brezzi condition, holds for the finite element discretizations of  $(\mathbf{u}_1, \mathbf{u}_2)$  and  $\boldsymbol{\lambda}$ . The lack of stability can have various consequences from minor reduction in the asymptotic convergence rate to a singular linear system. Moreover, the instability may manifest itself only for specific mesh configurations.

In dealing with mortar finite element methods, this has led to the development of special finite element techniques aiming at proving uniform stability independently of the finite element mesh. These techniques include adding additional bubble degrees-of-freedom for the displacement field [2], special biorthogonal finite element bases for the Lagrange multiplier [3], local modification of basis functions at the boundary of the

interface  $\Gamma$  [4], or stabilization of the bilinear form [5]. For instance, by adding stabilization terms one may use any conforming Lagrange multiplier spaces because the discrete norm, in which uniform stability can be established, arises naturally from the bilinear form.

Based on the abundance of literature on such special stabilization techniques, it could be easily inferred that they are absolutely necessary for successful approximation of tie contact problems. However, from a practical viewpoint, it is important to consider also low order finite elements in standard mixed variational formulation and their stability criteria. For instance, it is well known that piecewise-constant Lagrange multiplier is not stable together with piecewise-linear primal variable [6] without stabilization. Moreover, continuous piecewise-linear elements for both the displacement and the Lagrange multiplier may require modifications at Dirichlet boundaries or at interface junctions between three or more subdomains [7, 8]. Fortunately, in contact mechanics one is less likely to encounter such configurations assuming that the bodies are not fixed right next to the contact interface.

The purpose of this work is to study the discretization of the saddle point problem (1) using conforming mixed and stabilized finite element methods and investigate the stability and convergence of the methods. We consider a problem motivated by tie contact with the contact boundary  $\Gamma$  separated from Dirichlet boundaries by Neumann boundary of nonzero measure – existing literature suggests that this is also a necessary condition for uniform stability of the mixed method [2, 8, 7]. We first present a stabilized method based on Barbosa–Hughes stabilization [9] which is proven stable for any conforming finite element spaces or boundary conditions. Next we consider a mixed method which uses a continuous Lagrange multiplier and show that it leads to a uniformly stable method given that certain criteria are satisfied by the finite element mesh. The stability is also demonstrated numerically and the methods are shown to yield similar results in two-dimensional test cases. Finally, we present three-dimensional numerical results using an implementation of the lowest order stable mixed method in Elmer [10].

## 2. Problem formulation

The boundary  $\partial\Omega_i$  is split into the Dirichlet part  $\Gamma_{D,i}$ , the Neumann part  $\Gamma_{N,i}$ ,  $i = 1, 2$ , and the interface  $\Gamma$  between the two domains  $\Omega_1$  and  $\Omega_2$ . We assume that  $\Gamma_{D,i}$  and  $\Gamma$  are always separated by  $\Gamma_{N,i}$  to avoid using the Lions–Magenes space  $H_0^{1/2}(\Gamma)$  [11]. Moreover, if  $\Gamma_{D,i}$  and  $\Gamma$  are not separated, then the finite element space associated with the Lagrange multiplier in the mixed formulation must be modified [2].

The strong formulation of the tie contact problem reads as follows:

$$-\operatorname{div} \boldsymbol{\sigma}(\mathbf{u}_i) = \mathbf{f} \quad \text{in } \Omega_i, \quad (2)$$

where

$$\boldsymbol{\sigma}(\mathbf{u}_i) = \frac{E}{2(1+\nu)} \boldsymbol{\varepsilon}(\mathbf{u}_i) + \frac{E\nu}{(1+\nu)(1-2\nu)} \operatorname{tr} \boldsymbol{\varepsilon}(\mathbf{u}_i) \mathbf{I}, \quad \boldsymbol{\varepsilon}(\mathbf{u}_i) = \frac{1}{2} (\nabla \mathbf{u}_i + \nabla \mathbf{u}_i^T), \quad (3)$$

and  $(E, \nu)$  are the material parameters (Young’s modulus and Poisson ratio). The formulation is complemented with fixed and zero traction boundary conditions

$$\mathbf{u}_i = \mathbf{0} \quad \text{on } \Gamma_{D,i}, \quad \boldsymbol{\sigma}(\mathbf{u}_i) \mathbf{n} = \mathbf{0} \quad \text{on } \Gamma_{N,i}, \quad (4)$$

and the interface conditions

$$\boldsymbol{\lambda} = \boldsymbol{\sigma}(\mathbf{u}_2) \mathbf{n} = -\boldsymbol{\sigma}(\mathbf{u}_1) \mathbf{n} \quad \text{on } \Gamma \quad (5)$$

guaranteeing the continuity of the traction across the interface  $\Gamma$ .

Let us define the function space  $V_i = \{\mathbf{w} \in H^1(\Omega_i)^d : \mathbf{w}|_{\Omega_{\Gamma_{D,i}}} = 0\}$  and the dual space  $\Lambda = (H^{1/2}(\Gamma)^d)'$  where  $d \in \{2, 3\}$  is the dimension of the domain and  $H^{1/2}(\Gamma)$  refers to the space of traces of functions in  $H^1(\Omega)$  on  $\Gamma$ . In the following, we use the shorthand notation  $\mathbf{u} = (\mathbf{u}_1, \mathbf{u}_2) \in V_1 \times V_2 = V$  and, consequently,  $(\mathbf{u}, \boldsymbol{\lambda}) = (\mathbf{u}_1, \mathbf{u}_2, \boldsymbol{\lambda}) \in V \times \Lambda$ . The variational formulation of (2)–(5) then reads as: find  $(\mathbf{u}, \boldsymbol{\lambda}) \in V \times \Lambda$  satisfying

$$\begin{cases} (\boldsymbol{\sigma}(\mathbf{u}_1), \boldsymbol{\varepsilon}(\mathbf{v}_1))_{\Omega_1} + \langle \boldsymbol{\lambda}, \mathbf{v}_1 \rangle = (\mathbf{f}, \mathbf{v}_1)_{\Omega_1} \\ (\boldsymbol{\sigma}(\mathbf{u}_2), \boldsymbol{\varepsilon}(\mathbf{v}_2))_{\Omega_2} - \langle \boldsymbol{\lambda}, \mathbf{v}_2 \rangle = (\mathbf{f}, \mathbf{v}_2)_{\Omega_2} \\ \langle \boldsymbol{\mu}, \mathbf{u}_1 - \mathbf{u}_2 \rangle = 0, \end{cases} \quad (6)$$

for every  $(\mathbf{v}, \boldsymbol{\mu}) \in V \times \Lambda$ . In (6),  $(\cdot, \cdot)_A$  denotes the  $L^2$ -inner product over the subdomain  $A \subset \Omega$  and  $\langle \cdot, \cdot \rangle$  is the  $H^{1/2}(\Gamma)^d$ -duality pairing. Equivalently, we write (6) as: find  $(\mathbf{u}, \boldsymbol{\lambda}) \in V \times \Lambda$  satisfying

$$\mathcal{B}(\mathbf{u}, \boldsymbol{\lambda}; \mathbf{v}, \boldsymbol{\mu}) = \mathcal{L}(\mathbf{v}) \quad \forall (\mathbf{v}, \boldsymbol{\mu}) \in V \times \Lambda, \quad (7)$$

where the bilinear form  $\mathcal{B} : (V \times \Lambda) \times (V \times \Lambda) \rightarrow \mathbb{R}$  and the linear form  $\mathcal{L} : V \rightarrow \mathbb{R}$  are defined as

$$\begin{aligned} \mathcal{B}(\mathbf{w}, \boldsymbol{\xi}; \mathbf{v}, \boldsymbol{\mu}) &= \sum_{i=1}^2 (\boldsymbol{\sigma}(\mathbf{w}_i), \boldsymbol{\varepsilon}(\mathbf{v}_i))_{\Omega_i} + \langle \boldsymbol{\mu}, \llbracket \mathbf{w} \rrbracket \rangle + \langle \boldsymbol{\xi}, \llbracket \mathbf{v} \rrbracket \rangle, \\ \mathcal{L}(\mathbf{v}) &= \sum_{i=1}^2 (\mathbf{f}, \mathbf{v}_i)_{\Omega_i}, \end{aligned}$$

and  $\llbracket \mathbf{w} \rrbracket = \mathbf{w}_1 - \mathbf{w}_2$  denotes the jump of the displacement across the interface  $\Gamma$ . Existence and uniqueness of (7) is standard and follows the steps laid out in [1].

### 3. Stabilized finite element method

Let  $\mathcal{T}_h^i$  be a computational mesh of the domain  $\Omega_i$ ,  $i = 1, 2$ , with the mesh parameter  $h$  and  $\mathcal{G}_h$  be the set of edges/facets of  $\mathcal{T}_h^1$  on the interface  $\Gamma$ . To introduce the stabilized finite element method, we define the discrete spaces

$$\begin{aligned} V_{h,i} &= \{\mathbf{w} \in V_i : \mathbf{w}|_T \in \mathcal{P}_k(T)^d \quad \forall T \in \mathcal{T}_h^i\}, \quad V_h = V_{h,1} \times V_{h,2}, \\ \Lambda_h &= \{\boldsymbol{\xi} \in \Lambda : \boldsymbol{\xi}|_E \in \mathcal{P}_l(E)^d \quad \forall E \in \mathcal{G}_h\}, \end{aligned}$$

where  $k \geq 1$  and  $l \geq 0$  are the polynomial degrees.

Let  $h_\Gamma \in L^2(\Gamma)$  be such that  $h_\Gamma|_E = h_E \quad \forall E \in \mathcal{G}_h$ , and let  $\alpha > 0$  be a stabilization parameter. The discrete bilinear form  $\mathcal{B}_h : (V_h \times \Lambda_h) \times (V_h \times \Lambda_h) \rightarrow \mathbb{R}$ , defined as

$$\mathcal{B}_h(\mathbf{w}, \boldsymbol{\xi}; \mathbf{v}, \boldsymbol{\mu}) = \mathcal{B}(\mathbf{w}, \boldsymbol{\xi}; \mathbf{v}, \boldsymbol{\mu}) - \alpha (h_\Gamma (\boldsymbol{\xi} + \boldsymbol{\sigma}(\mathbf{w}_1)\mathbf{n}), \boldsymbol{\mu} + \boldsymbol{\sigma}(\mathbf{v}_1)\mathbf{n})_\Gamma, \quad (8)$$

is continuous and stable in the following mesh-dependent norm (see Theorem 1 below):

$$\| \! \| (\mathbf{w}, \boldsymbol{\xi}) \| \! \|_h^2 = \| \! \| \mathbf{w} \| \! \| ^2 + \| h_\Gamma^{1/2} \boldsymbol{\xi} \|_{0,\Gamma}^2. \quad (9)$$

Note that (8) is stabilized using the residual of (5). In (9), the norm for the displacement is given by the strain energy:

$$\| \! \| \mathbf{w} \| \! \| ^2 = \sum_{i=1}^2 (\boldsymbol{\sigma}(\mathbf{w}_i), \boldsymbol{\varepsilon}(\mathbf{w}_i))_{\Omega_i}.$$

The stabilized finite element formulation now reads as follows: find  $(\mathbf{u}_h, \boldsymbol{\lambda}_h) \in V_h \times \Lambda_h$  satisfying

$$\mathcal{B}_h(\mathbf{u}_h, \boldsymbol{\lambda}_h; \mathbf{v}, \boldsymbol{\mu}) = \mathcal{L}(\mathbf{v}) \quad \forall (\mathbf{v}, \boldsymbol{\mu}) \in V_h \times \Lambda_h.$$

The stability of the formulation is proved in the following theorem.

**Theorem 1.** *For small enough  $\alpha > 0$  and any  $(\mathbf{w}, \boldsymbol{\xi}) \in V_h \times \Lambda_h$  there exists  $C > 0$ , independent of  $h$ , such that*

$$\mathcal{B}_h(\mathbf{w}, \boldsymbol{\xi}; \mathbf{w}, -\boldsymbol{\xi}) \geq C \| \! \| (\mathbf{w}, \boldsymbol{\xi}) \| \! \|_h^2.$$

*Proof.* The definition of the form  $\mathcal{B}_h$  in (8) and the discrete trace estimate (see, e.g., [12])

$$C_I \| h_\Gamma^{1/2} \boldsymbol{\sigma}(\mathbf{w}_1)\mathbf{n} \|_{0,\Gamma}^2 \leq (\boldsymbol{\sigma}(\mathbf{w}_1), \boldsymbol{\varepsilon}(\mathbf{w}_1))_{\Omega_1},$$

where  $C_I$  is independent of  $h$ , imply that for any  $(\mathbf{w}, \boldsymbol{\xi}) \in V_h \times \Lambda_h$  it holds

$$\begin{aligned} \mathcal{B}_h(\mathbf{w}, \boldsymbol{\xi}; \mathbf{w}, -\boldsymbol{\xi}) &= \|\!(\mathbf{w}, \boldsymbol{\xi})\|_h^2 - \alpha \|h_\Gamma^{1/2} \boldsymbol{\sigma}(\mathbf{w}_1) \mathbf{n}\|_{0,E}^2 \\ &\geq \left(1 - \frac{\alpha}{C_I}\right) \|\mathbf{w}\|^2 + \alpha \|h_\Gamma^{1/2} \boldsymbol{\xi}\|_{0,\Gamma}^2. \end{aligned}$$

The terms on the right hand side remain positive if  $0 < \alpha < C_I$ .  $\square$

**Remark 1.** From the proof of Theorem 1, it is obvious that the result holds for any conforming Lagrange multiplier space, continuous or discontinuous. One may even use non-local functions to define a global spectral basis. This idea has been used, e.g., in Hansbo [13] to simplify the implementation and circumvent the need for a conforming integration mesh. Moreover, it is possible to eliminate a discontinuous, piecewise polynomial Lagrange multiplier locally on each element to arrive at a positive definite Nitsche-type method [14, 5, 12].

As a consequence of Theorem 1, we have the following quasi-optimality estimate:

**Theorem 2.** *Suppose  $\mathbf{u} \in H^{3/2}(\Omega_1)^d \times H^{3/2}(\Omega_2)^d$ . There exists  $C > 0$  such that*

$$\|\!(\mathbf{u} - \mathbf{u}_h, \boldsymbol{\lambda} - \boldsymbol{\lambda}_h)\|_h \leq C \inf_{\substack{(\mathbf{v}_h, \boldsymbol{\mu}_h) \\ \in V_h \times \Lambda_h}} \|\!(\mathbf{u} - \mathbf{v}_h, \boldsymbol{\lambda} - \boldsymbol{\mu}_h)\|_h.$$

*Proof.* Discrete stability (Theorem 1), the orthogonality result

$$\mathcal{B}_h(\mathbf{u} - \mathbf{u}_h, \boldsymbol{\lambda} - \boldsymbol{\lambda}_h; \mathbf{v}_h, \boldsymbol{\mu}_h) = 0 \quad \forall (\mathbf{v}_h, \boldsymbol{\mu}_h) \in V_h \times \Lambda_h,$$

and continuity of  $\mathcal{B}_h$ , imply that

$$\begin{aligned} &\|\!(\mathbf{u}_h - \mathbf{v}_h, \boldsymbol{\lambda}_h - \boldsymbol{\mu}_h)\|_h^2 \\ &\leq C \mathcal{B}_h(\mathbf{u}_h - \mathbf{v}_h, \boldsymbol{\lambda}_h - \boldsymbol{\mu}_h; \mathbf{u}_h - \mathbf{v}_h, \boldsymbol{\lambda}_h - \boldsymbol{\mu}_h) \\ &= C \mathcal{B}_h(\mathbf{u} - \mathbf{v}_h, \boldsymbol{\lambda} - \boldsymbol{\mu}_h; \mathbf{u}_h - \mathbf{v}_h, \boldsymbol{\lambda}_h - \boldsymbol{\mu}_h) \\ &\leq C \|\!(\mathbf{u} - \mathbf{v}_h, \boldsymbol{\lambda} - \boldsymbol{\mu}_h)\|_h \|\!(\mathbf{u}_h - \mathbf{v}_h, \boldsymbol{\lambda}_h - \boldsymbol{\mu}_h)\|_h. \end{aligned}$$

Dividing both sides by  $\|\!(\mathbf{u}_h - \mathbf{v}_h, \boldsymbol{\lambda}_h - \boldsymbol{\mu}_h)\|_h$  and using the triangle inequality leads to the proof.  $\square$

**Remark 2.** It is possible to prove Theorem 1 in the  $V$ -norm for the displacement and in the continuous  $H^{-1/2}(\Gamma)$ -norm for the Lagrange multiplier, to arrive at a similar estimate without extra regularity assumptions [14].

#### 4. Mixed finite element method

Let us next consider a mixed method using a continuous Lagrange multiplier, i.e. the spaces

$$\begin{aligned} V_{h,i} &= \{\mathbf{w} \in V_i : \mathbf{w}|_T \in \mathcal{P}_k(T)^d \ \forall T \in \mathcal{T}_h^i\}, \quad V_h = V_{h,1} \times V_{h,2}, \\ \Lambda_h^c &= \{\boldsymbol{\xi} \in \Lambda \cap C(\Gamma)^d : \boldsymbol{\xi}|_E \in \mathcal{P}_l(E)^d \ \forall E \in \mathcal{G}_h\} \end{aligned} \tag{10}$$

where  $k, l \geq 1$ . This approach is mentioned in the early work of Pitkäranta [15] where it is noted that the discrete stability holds if the space of Lagrange multipliers is a subset of the trace space of  $V_{h,1}$ . However, the stability may not, in general, be uniform in  $h$  without additional restrictions on the finite element mesh.

The discrete mixed formulation reads as follows: find  $(\mathbf{u}_h, \boldsymbol{\lambda}_h) \in V_h \times \Lambda_h^c$  satisfying

$$\mathcal{B}(\mathbf{u}_h, \boldsymbol{\lambda}_h; \mathbf{v}, \boldsymbol{\mu}) = \mathcal{L}(\mathbf{v}) \quad \forall (\mathbf{v}, \boldsymbol{\mu}) \in V_h \times \Lambda_h^c.$$

The Babuška–Brezzi condition, guaranteeing stability is written as: there exists  $C > 0$ , independent of  $h$ , such that

$$\sup_{\mathbf{v}_h \in V_h} \frac{\langle \llbracket \mathbf{v}_h \rrbracket, \boldsymbol{\xi}_h \rangle}{\|\mathbf{v}_h\|} \geq C \|\boldsymbol{\xi}_h\|_{-\frac{1}{2}} \quad \forall \boldsymbol{\xi}_h \in \Lambda_h^c. \quad (11)$$

Here we establish the uniform stability for the mixed method using the mesh-dependent norm in  $\Lambda_h^c$  and the following auxiliary result [14].

**Lemma 1.** *If there exists  $C > 0$ , independent of  $h$ , such that*

$$\sup_{\mathbf{v}_h \in V_h} \frac{\langle \llbracket \mathbf{v}_h \rrbracket, \boldsymbol{\xi}_h \rangle}{\|\mathbf{v}_h\|} \geq C \|h_\Gamma^{1/2} \boldsymbol{\xi}_h\|_{0,\Gamma}^2 \quad \forall \boldsymbol{\xi}_h \in \Lambda_h^c, \quad (12)$$

*then the Babuška–Brezzi condition (11) holds.*

Lemma 1 can be proven independently of the finite element spaces for any shape regular mesh families using the stability of the continuous problem and Clément interpolation, see [14]. The following assumption on the finite element meshes  $(\mathcal{T}_h^1, \mathcal{T}_h^2, \mathcal{G}_h)$  is sufficient for stability in the mesh-dependent norm, see [16] for a discussion on similar estimates with graded meshes.

**Assumption 1.** *The  $L^2$ -projection  $\pi_h : L^2(\Gamma)^d \rightarrow \Lambda_h^c$  satisfies*

$$\|h_\Gamma^{-1/2} \pi_h \mathbf{v}\|_{0,\Gamma} \leq C \|h_\Gamma^{-1/2} \mathbf{v}\|_{0,\Gamma} \quad \forall \mathbf{v} \in L^2(\Gamma)^d.$$

**Theorem 3.** *If  $k = l = 1$  in (10) and the finite element mesh satisfies Assumption 1 then the stability condition (12) holds.*

*Proof.* Let  $\mathcal{E}_h \boldsymbol{\xi}_h$ , where  $\mathcal{E}_h : \Lambda_h^c \rightarrow V_{h,1}$ , be the extension of a piecewise linear function  $\boldsymbol{\xi}_h$  on  $\Gamma$  to  $\Omega_1$  defined via the finite element basis so that the nodes outside of the interface  $\Gamma$  have value zero. For such an extension it holds [17]

$$\|\nabla \mathcal{E}_h \boldsymbol{\mu}_h\|_{0,\Omega_1}^2 \leq C_E \|h_\Gamma^{-1/2} \boldsymbol{\mu}_h\|_{0,\Gamma}^2 \quad \forall \boldsymbol{\mu}_h \in \Lambda_h^c. \quad (13)$$

From the definition of the  $L^2$ -projection, choosing  $\mathbf{w}_h = (\mathbf{w}_{1,h}, 0) = (\mathcal{E}_h \pi_h(h_\Gamma \boldsymbol{\xi}_h), 0)$ , it follows that

$$\langle \llbracket \mathbf{w}_h \rrbracket, \boldsymbol{\xi}_h \rangle = \langle \pi_h(h_\Gamma \boldsymbol{\xi}_h), \boldsymbol{\xi}_h \rangle = \|h_\Gamma^{1/2} \boldsymbol{\xi}_h\|_{0,\Gamma}^2. \quad (14)$$

Using Korn's inequality, property (13) and Assumption 1, we obtain

$$\begin{aligned} \|\mathbf{w}_h\|^2 &= (\boldsymbol{\sigma}(\mathbf{w}_{1,h}), \boldsymbol{\varepsilon}(\mathbf{w}_{1,h})_{\Omega_1}) \\ &\leq C_K \|\nabla \mathcal{E}_h \pi_h(h_\Gamma \boldsymbol{\xi}_h)\|_{0,\Omega_1}^2 \\ &\leq C_K C_E \|h_\Gamma^{-1/2} \pi_h(h_\Gamma \boldsymbol{\xi}_h)\|_{0,\Gamma}^2 \\ &\leq C_K C_E C \|h_\Gamma^{1/2} \boldsymbol{\xi}_h\|_{0,\Gamma}^2. \end{aligned} \quad (15)$$

The result now follows from (14) and (15).  $\square$

**Remark 3.** As a stronger alternative to Assumption 1, we can assume that there exist  $C_1, C_2 > 0$ , independent of  $h$ , satisfying

$$C_1 \min_{F \in \mathcal{G}_h} h_F \leq h_E \leq C_2 \max_{F \in \mathcal{G}_h} h_F \quad \forall E \in \mathcal{G}_h. \quad (16)$$

Unfortunately, (16) requires the mesh to be uniform.

**Remark 4.** For  $P_k - P_{k-1}$ ,  $k \geq 2$ , the proof of Theorem 3 can be adapted, see also [18] where similar methods are discussed for multiple subdomains. For  $P_k - P_{k-2}$ ,  $k \geq 2$ , with a discontinuous Lagrange multiplier, the proof simplifies in 2D because we can use the edge bubbles of  $P_k$  on  $\Gamma$ .

## 5. Numerical experiments

In this section, we perform experiments using both methods and different polynomial orders. We refer to the method using polynomial order  $k$  for the displacement and  $l$  for the continuous Lagrange multiplier as  $P_k - P_l$  mixed method. The two-dimensional examples are implemented using scikit-fem [19] and visualized using matplotlib [20] whereas the three-dimensional examples are implemented using the finite element software Elmer [10] and visualized using Paraview [21]. In all examples the material parameters are taken to be  $E = 10^3$  and  $\nu = 0.3$  in both bodies.

### 5.1. Square against square, unstable example

For completeness, we first demonstrate the instability of  $P_1 - P_0$  mixed method and how stabilization recovers the expected rate of convergence. The domain is

$$\Omega_1 \cup \Omega_2 = (0, 1)^2 \cup (1, 1.5) \times (0, 1).$$

The boundaries are

$$\Gamma_{D,1} = \{(0, y) : 0 < y < 1\}, \quad \Gamma_{D,2} = \{(1.5, y) : 0 < y < 1\}, \quad \Gamma_{N,i} = \partial\Omega_i \setminus (\Gamma_{D,i} \cup \Gamma),$$

and the essential boundary conditions are

$$\mathbf{u}_1|_{\Gamma_{D,1}} = (0.1, 0), \quad \mathbf{u}_2|_{\Gamma_{D,2}} = (0, 0).$$

The instability of  $P_1 - P_0$  mixed method with a piecewise constant Lagrange multiplier is clearly visible when using matching vertices. The initial meshes are given in Figure 1. The Lagrange multipliers are visualized in Figure 2 from which it becomes clear that the tangential Lagrange multiplier does not properly represent the true solution. This is further exemplified in Figure 3 (left) where we observe that the convergence rate of the Lagrange multiplier is seriously affected by the lack of stabilization.

For the stabilized method, we observe superconvergence of the Lagrange multiplier with the error of the order  $\mathcal{O}(h^{3/2})$  – instead of  $\mathcal{O}(h)$  as suggested by the linear approximation of the primal variable. The reference solution was calculated using a stabilized  $P_3 - P_2$  method and a very fine mesh.

### 5.2. Square against square, $P_1 - P_1$ methods

In order to demonstrate the stability of the mixed  $P_1 - P_1$  method, we solve the same problem as above using both the mixed method and its stabilized counterpart using a continuous Lagrange multiplier. A nonmatching mesh is used to demonstrate the approach in the case of general meshes. The convergence rates are in Figure 3 (right) and the Lagrange multipliers are visualized in Figure 5. As a conclusion, both methods give essentially the same results. As above, we observe superconvergence of the Lagrange multiplier with the error of order  $\mathcal{O}(h^2)$ .

### 5.3. Three-dimensional examples

The mixed  $P_1 - P_1$  method is implemented in Elmer [10] for three-dimensional geometry. We first present an example where a cylinder with the radius and height of 0.5 and 1, respectively, is pushed against a cube with side length of 1, see Figure 6. The external force is introduced through inhomogeneous Dirichlet boundary condition, i.e. the bottom surface of the block is fixed whereas the top surface of the cylinder is forced downwards 0.1 units. Consequently, the exact solution is independent of the cylinder's axial rotation and the discrete problem can be solved using several angles to observe how the orientation of elements affects the contact force.

The cylinder is discretized using linear tetrahedral elements in Gmsh [22] and the block is discretized using trilinear hexahedral tensor product grid. The normal and tangential components of the contact force are given for three different values of cylinder's axial rotation ( $0$ ,  $\pi/6$  and  $\pi/3$ ) in Figures 7 and 8. All rotation angles lead to practically identical normal and tangential contact forces which suggests that the method is robust with respect to the shape and the orientation of the elements at the contact interface.

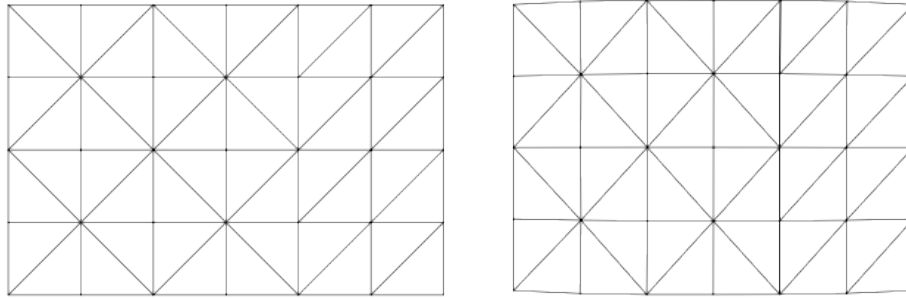


Figure 1: The initial meshes (left) and the deformed meshes (right) with matching nodes for the first numerical experiment.

The second three-dimensional example concerns a more complicated geometry with a cylindrical shaft cutting through a block. The cylinder has radius 0.25 and height 1, and the block is a cube with side length of 1, see Figure 9. The block is squeezed 0.1 units using a similar boundary condition as before. The cylinder is rotated around its axis and results are obtained for several angles of rotation. The contact forces are given in Figures 10 and 11 demonstrating once again the independence of the results on the finite element mesh.

The final example is a three-dimensional version of the convergence study in Section 5.2. More precisely, a cubical block with side length of 1 is pushed downward against another block with same horizontal dimensions and of height 0.5. As we do not possess a sufficiently accurate reference solution, we compute the strain energy at different mesh refinement levels and visualize its change as a function of the mesh parameter, see Figure 14 where a linear rate is demonstrated. The corresponding contact forces are shown in Figures 12 and 13.

## 6. Discussion

Mortar finite element methods are naturally presented in a mixed variational formulation and these methods often use special finite element bases. In this paper, we have presented two finite element formulations, mixed and stabilized, for the approximation of the elastic tie contact problem. Both use standard finite elements and are stable for continuous  $P_1 - P_1$  elements, the mixed method under certain mild assumptions on the boundary conditions and the finite element mesh. Furthermore, the stabilized formulation allows using any conforming continuous or discontinuous Lagrange multiplier approximation. The numerical experiments, both 2D and 3D, corroborate the stability of the methods.

## Acknowledgements

The work was supported by the Academy of Finland (Decisions 324611 and 338341) and the Portuguese government through FCT (Fundação para a Ciência e a Tecnologia), I.P., under the projects PTDC/MAT-PUR/28686/2017 and UIDB/04459/2020.

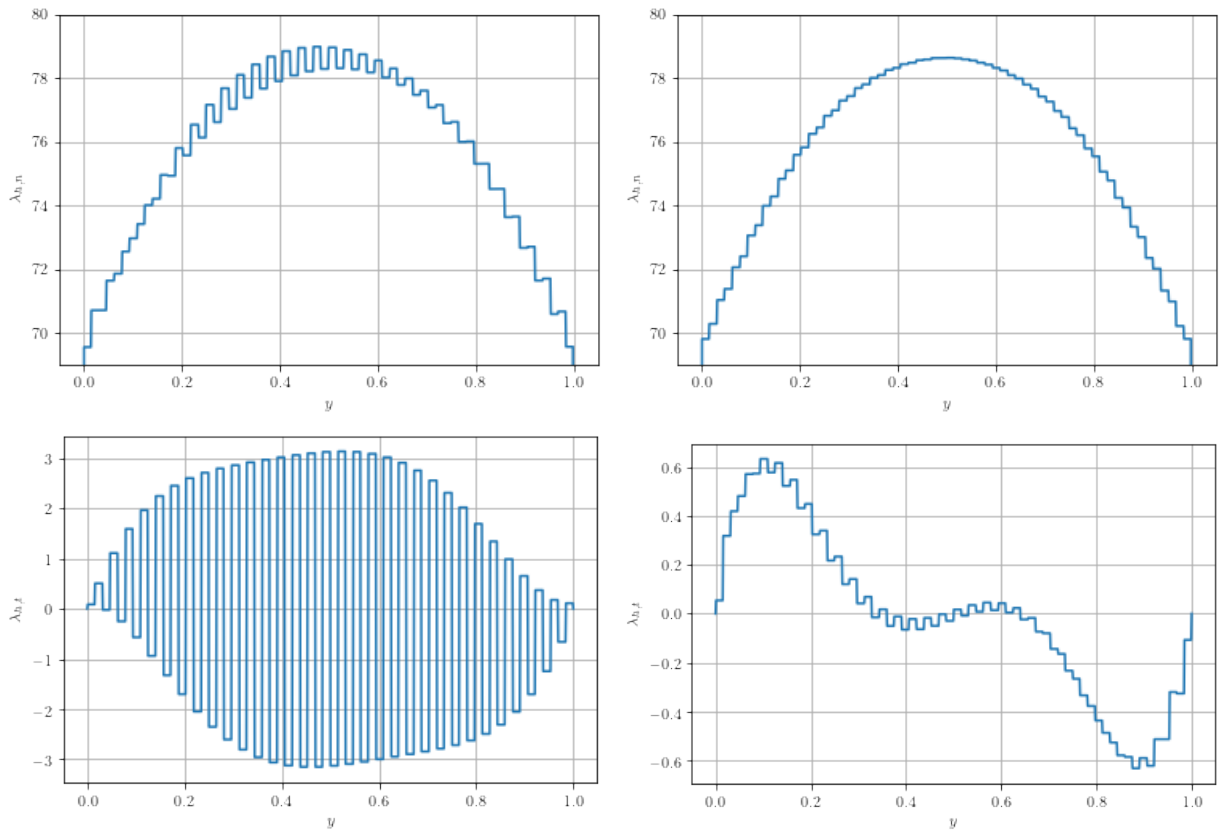


Figure 2: A comparison of the Lagrange multipliers for the unstable  $P_1 - P_0$  mixed method (left) and its stabilized counterpart (right).

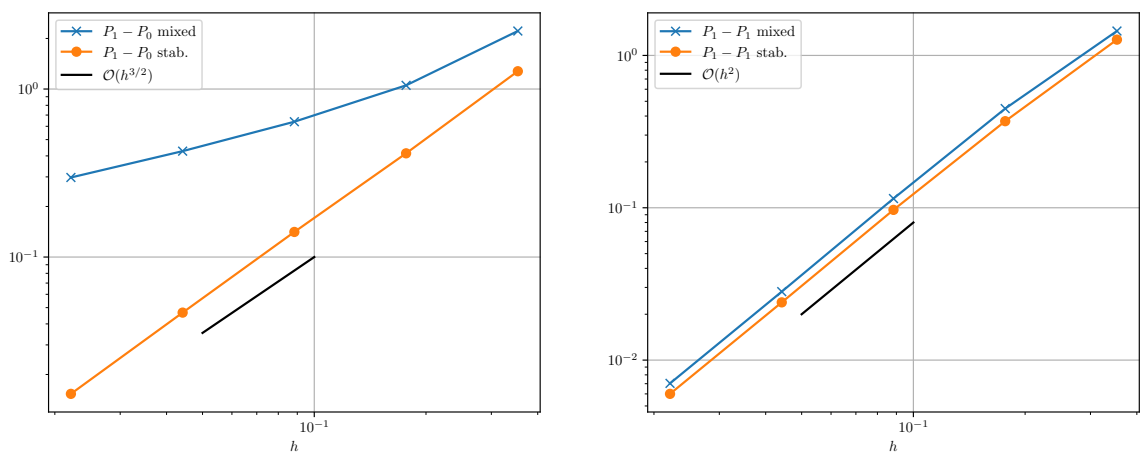


Figure 3: The error of the Lagrange multiplier for  $P_1 - P_0$  methods (left) and  $P_1 - P_1$  methods (right) in the discrete  $H^{-1/2}$ -norm.



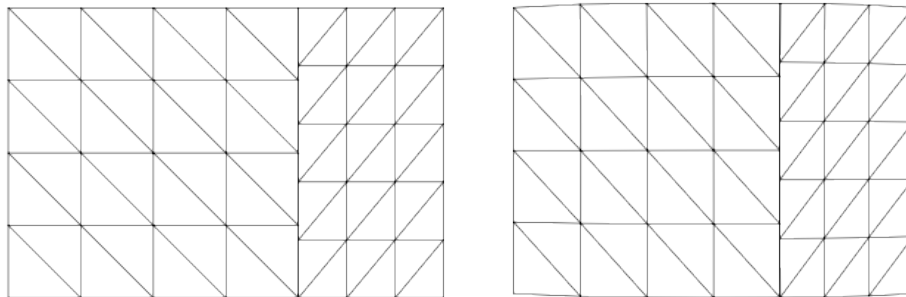


Figure 4: The initial meshes (left) and the deformed meshes (right) with nonmatching nodes for the second numerical experiment.

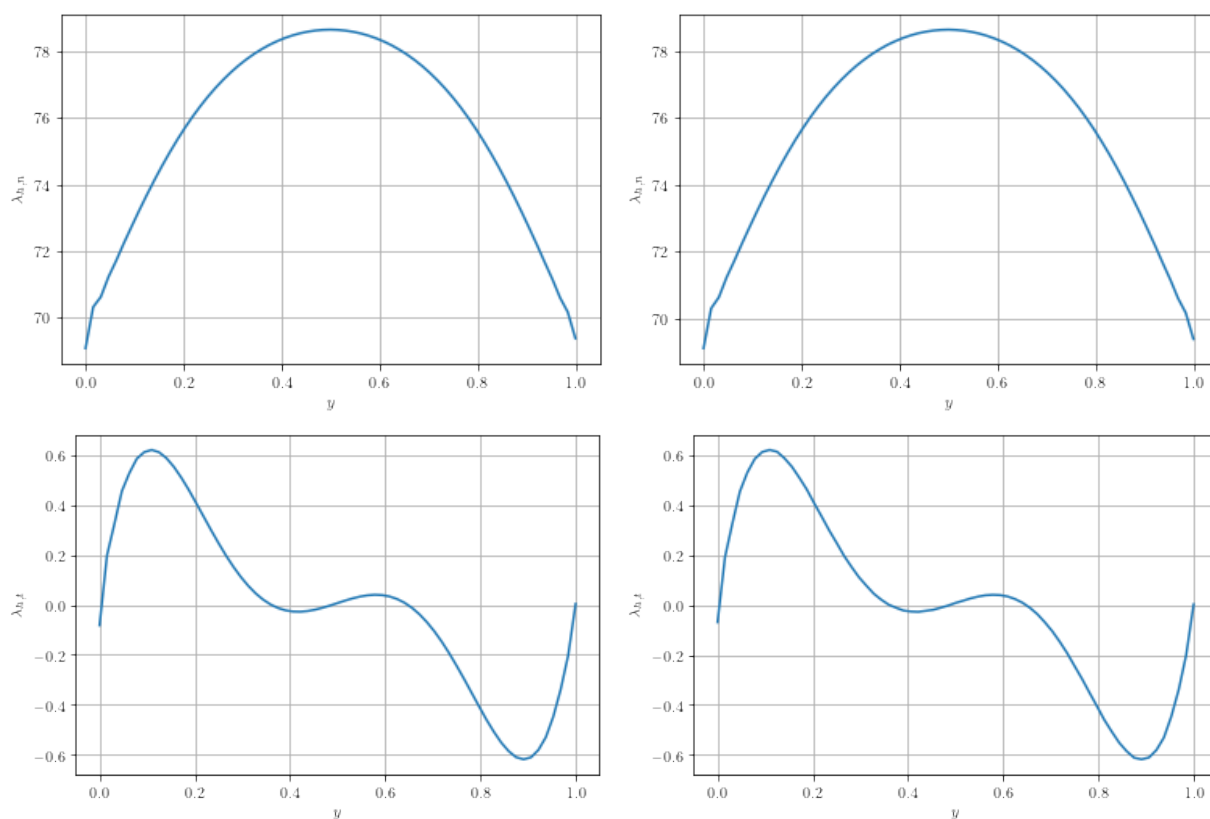


Figure 5: A comparison of the Lagrange multipliers for the mixed (left) and stabilized (right)  $P_1 - P_1$  methods.

## References

- [1] I. Babuška, The finite element method with Lagrangian multipliers, *Numerische Mathematik* 20 (3) (1973) 179–192.
- [2] P. Hauret, M. Ortiz, BV estimates for mortar methods in linear elasticity, *Computer methods in applied mechanics and engineering* 195 (37-40) (2006) 4783–4793.
- [3] B. I. Wohlmuth, A mortar finite element method using dual spaces for the Lagrange multiplier, *SIAM journal on numerical analysis* 38 (3) (2000) 989–1012.
- [4] C. Bernardi, Y. Maday, A. T. Patera, Domain decomposition by the mortar element method, in: *Asymptotic and numerical methods for partial differential equations with critical parameters*, Springer, 1993, pp. 269–286.
- [5] T. Gustafsson, R. Stenberg, J. Videman, Error analysis of Nitsche’s mortar method, *Numerische Mathematik* 142 (4) (2019) 973–994.
- [6] B. Wohlmuth, Variationally consistent discretization schemes and numerical algorithms for contact problems, *Acta Numerica* 20 (2011) 569–734.
- [7] F. B. Belgacem, The mortar finite element method with Lagrange multipliers, *Numerische Mathematik* 84 (2) (1999) 173–197.
- [8] F. B. Belgacem, P. Hild, P. Laborde, The mortar finite element method for contact problems, *Mathematical and Computer Modelling* 28 (4-8) (1998) 263–271.
- [9] H. J. Barbosa, T. J. Hughes, The finite element method with Lagrange multipliers on the boundary: circumventing the Babuška-Brezzi condition, *Computer Methods in Applied Mechanics and Engineering* 85 (1) (1991) 109–128.
- [10] M. Malinen, P. Råback, Elmer finite element solver for multiphysics and multiscale problems, *Multiscale Model. Methods Appl. Mater. Sci.* 19 (2013) 101–113.
- [11] L. Tartar, *An introduction to Sobolev spaces and interpolation spaces*, Vol. 3, Springer Science & Business Media, 2007.
- [12] T. Gustafsson, R. Stenberg, J. Videman, On Nitsche’s method for elastic contact problems, *SIAM Journal on Scientific Computing* 42 (2) (2020) B425–B446.
- [13] P. Hansbo, Nitsche’s method for interface problems in computational mechanics, *GAMM-Mitteilungen* 28 (2) (2005) 183–206.
- [14] T. Gustafsson, R. Stenberg, J. Videman, Mixed and stabilized finite element methods for the obstacle problem, *SIAM Journal on Numerical Analysis* 55 (6) (2017) 2718–2744.
- [15] J. Pitkäranta, Boundary subspaces for the finite element method with Lagrange multipliers, *Numerische Mathematik* 33 (3) (1979) 273–289.
- [16] R. E. Bank, H. Yserentant, On the  $H^1$ -stability of the  $L^2$ -projection onto finite element spaces, *Numerische Mathematik* 126 (2) (2014) 361–381.
- [17] R. Verfürth, *A Posteriori Error Estimation Techniques for Finite Element Methods*, Oxford University Press, 2013. doi: 10.1093/acprof:oso/9780199679423.001.0001.
- [18] P. Seshaiyer, M. Suri, Uniform  $hp$  convergence results for the mortar finite element method, *Mathematics of Computation* 69 (230) (2000) 521–546.
- [19] T. Gustafsson, G. D. McBain, scikit-fem: A Python package for finite element assembly, *Journal of Open Source Software* 5 (52) (2020) 2369. doi:10.21105/joss.02369.
- [20] J. D. Hunter, Matplotlib: A 2d graphics environment, *Computing in science & engineering* 9 (03) (2007) 90–95.
- [21] J. Ahrens, B. Geveci, C. Law, Paraview: An end-user tool for large data visualization, *The visualization handbook* 717 (8) (2005).
- [22] C. Geuzaine, J.-F. Remacle, Gmsh: A 3-d finite element mesh generator with built-in pre-and post-processing facilities, *International journal for numerical methods in engineering* 79 (11) (2009) 1309–1331.

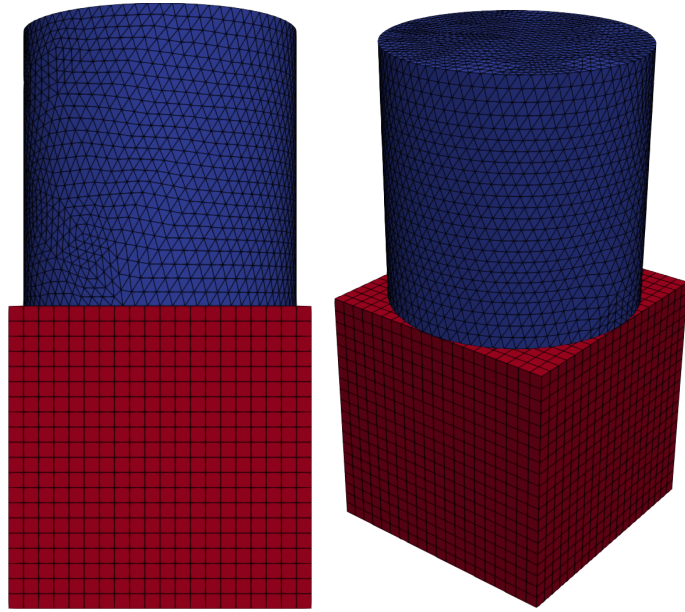


Figure 6: Cylinder and block geometry and computational mesh.

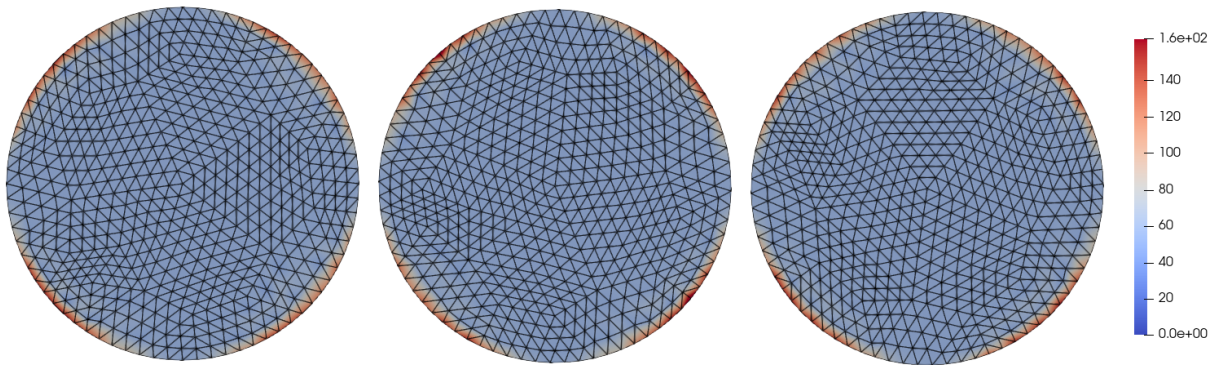


Figure 7: The normal contact loads for three different angles.

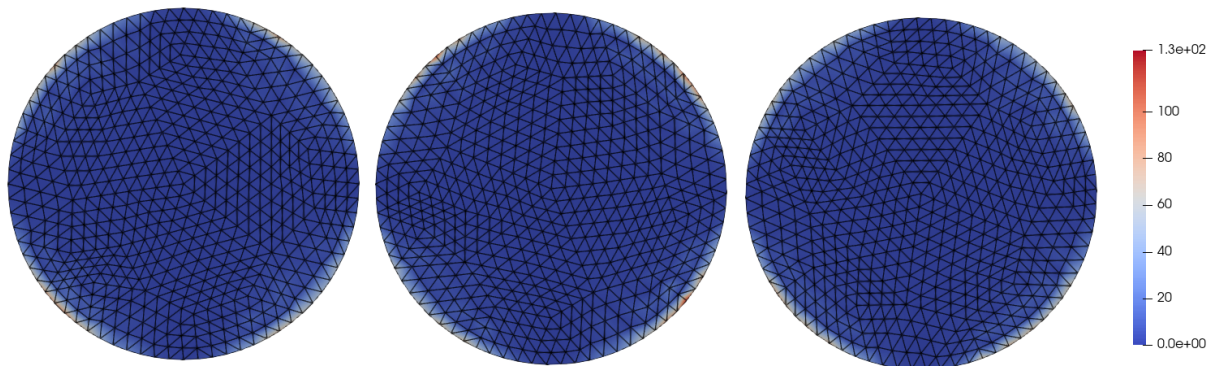


Figure 8: The tangential contact load magnitudes for three different angles.

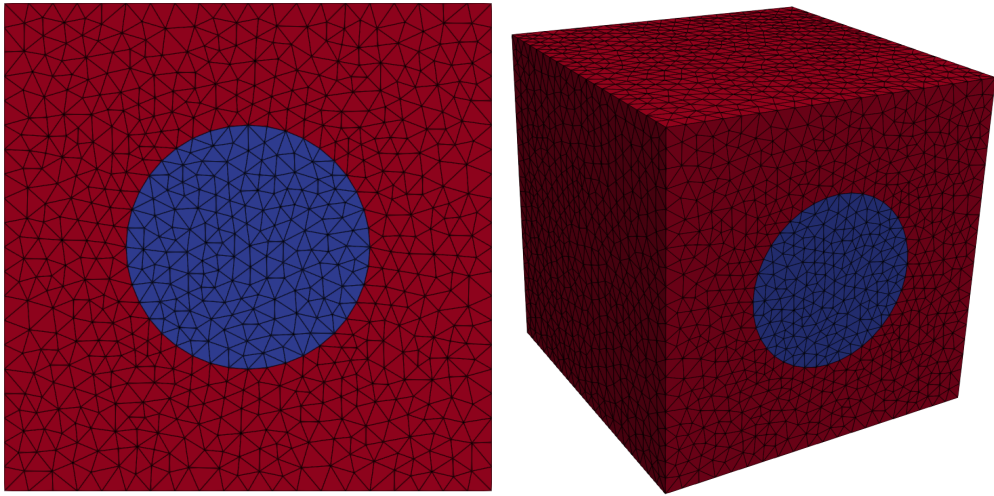


Figure 9: Cylinder cutting the cube.

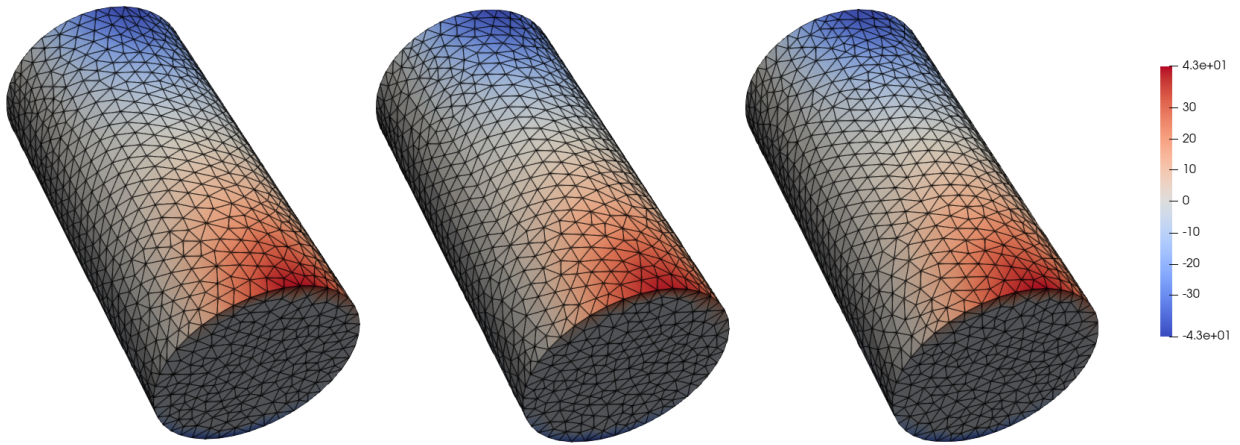


Figure 10: The normal contact loads for three different angles.

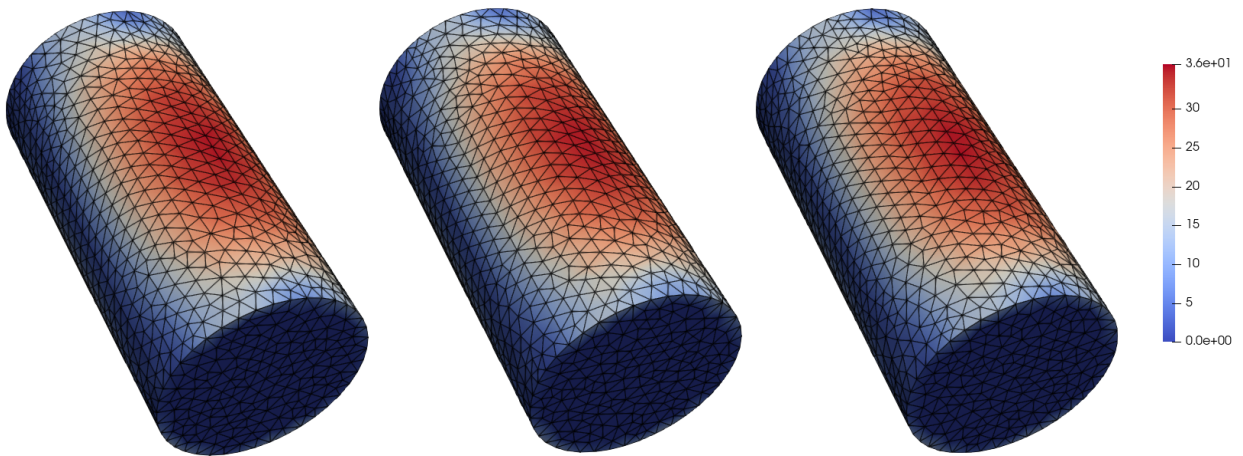


Figure 11: The tangential contact load magnitudes for three different angles.

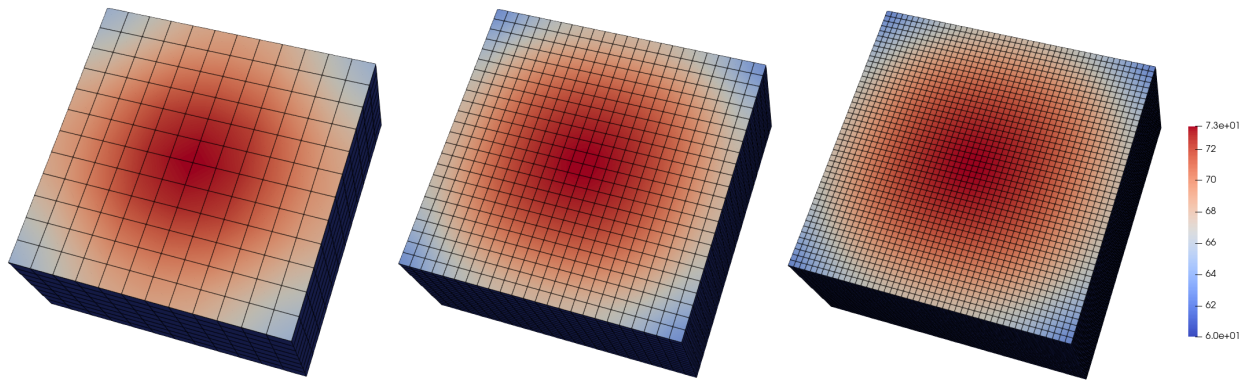


Figure 12: The normal contact loads for three different refinement levels.

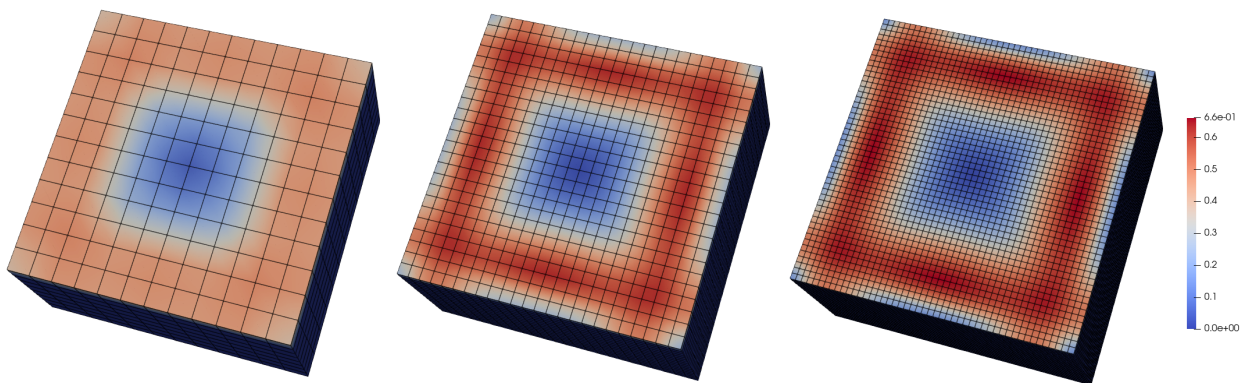


Figure 13: The tangential contact load magnitudes for three different refinement levels.

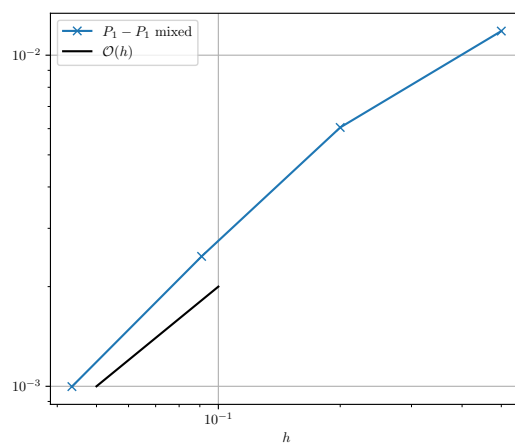


Figure 14: The absolute change in the strain energy between two subsequent refinement levels as a function of the mesh parameter  $h$ .